

7

Fabrication of Nanoporous Alumina

R. Abdel-Karim*, S. M. El-Raghy

Dept. of Metallurgy, Faculty of Engineering, Cairo University, Giza 12613, Egypt

*Corresponding author

Outline:

Introduction.....	198
Anodic aluminium oxide	200
<i>Types of anodic oxides of aluminium</i>	201
<i>Types of anodization process</i>	202
Thermodynamics of aluminium anodizing process	204
Formation and growth mechanisms of anodic porous alumina	205
Kinetics of Oxide Formation and Oxide Dissolution	209
Influence of electrochemical conditions on porous anodized alumina	210
Applications of Porous Anodic Alumina	213
Conclusion.....	214
References.....	215

Introduction

Nanostructured metal oxide material devices have exhibited many high-tech applications^[1] such as dye-sensitized solar cells^[2], displays and smart windows^[3], biosensors^[4], lithium batteries^[5], and super capacitors^[6]. In order to fulfil the great promise and expectation of nanomaterials, a number of new synthetic techniques and patterning methods have been developed, such as self-assembly^[7], mechanochemistry^[8], chemistry by microwave^[4], lithography^[5] or template- and membrane-based synthesis^[9-11].

Among these methods, the anodizing approach is able to build metal oxide nanopores of controllable pore size, good uniformity, array-orderly, and conformability over large areas at low cost via a simple electrochemical experimental procedure^[1].

Inspired by the success of porous alumina membrane, great attention has been paid to other metals, or valve metals, such as titanium, hafnium niobium that are capable of synthesizing ordered nanostructured metal oxides with unique physical and chemical properties^[1]. The term "valve metals" for that group of elements dates from an early research period which stressed the characteristic property of rectification of these oxide coated metals in most electrolytes (the forward direction is cathodic). Under reverse-bias, the anodic current flowing is generally due to growth of the surface oxide film by ionic transport^[12]. Owing to their low electrochemical potential the group IVB and VB valve metals Ti, Zr, Hf, V, Nb and Ta readily react with water or oxygen to form a dense, protecting passive layer, which also holds for Al^[13].

The most significant difference between typical anodic titanium oxide and anodic aluminium oxide is that the latter is a continuous film with a pore array while the former consists of separated nanotubes as demonstrated. Applications: photo catalysis, gas sensors, photo electrolysis and photovoltaics (Figure 7.1)^[14].

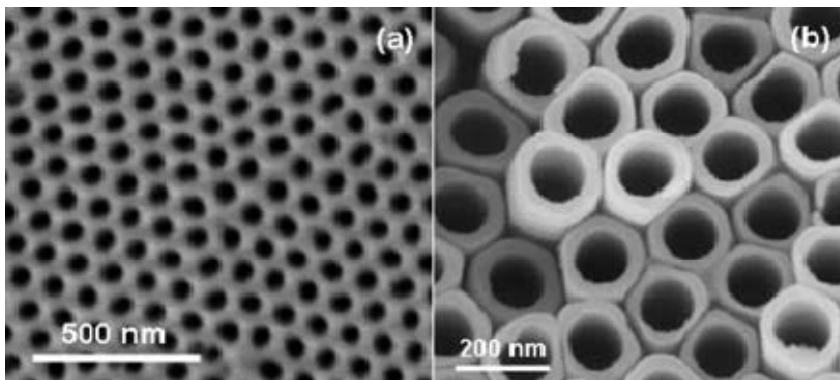


FIGURE 7.1
FE-SEM images of (a) anodic aluminium oxide film and (b) titanium oxide nanotubes^[14]

Anodic Hafnium oxide has many interesting properties, e.g. its high chemical and thermal stabilities, high refractive index and relatively high dielectric constant. Anodization potential was found to be a key factor affecting the morphology and the structure of the porous oxide. The pore diameter was found to increase with increasing potential (Figure 7.2). Applications: used as a protective coating, optical coating, gas sensor or capacitor^[15].

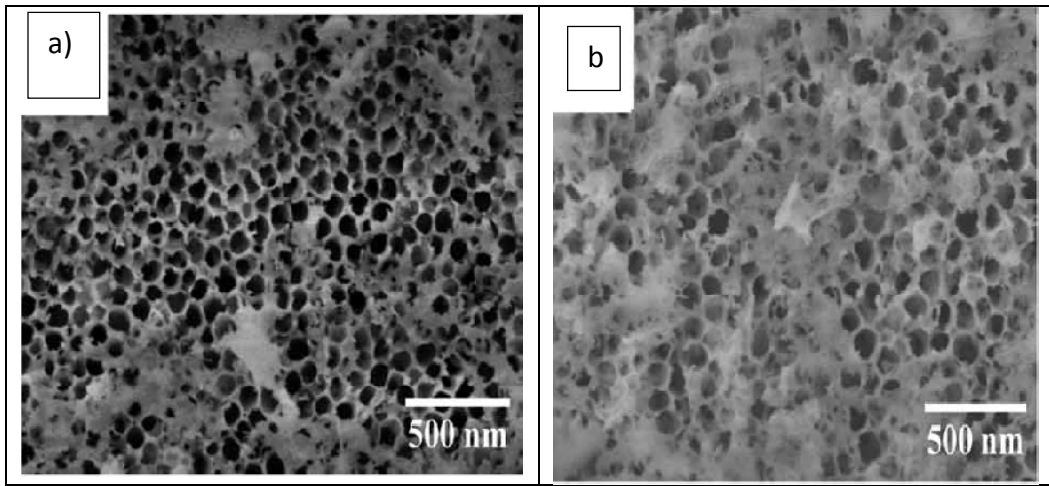


FIGURE 7.2

FE-SEM images of anodic porous hafnium oxide layers formed as a function of applied potential in 1 M H_2SO_4 + 0.04 M NaF at room temperature; (a) 50 V and (b) 60 V^[15]

Porous niobium oxide structures could be applied in gas sensors, catalysis, and optical and electrochromic devices. Anodization of niobium has been studied in various electrolytes^[16]. Choi et al^[16] obtained anodic Nb_2O_5 films with an effective thickness over 500 nm, consisting of a protective outer layer of around 90–130 nm and an inner layer of 300–400 nm, via an optimized anodization–annealing–anodization process (Figure 7.4).

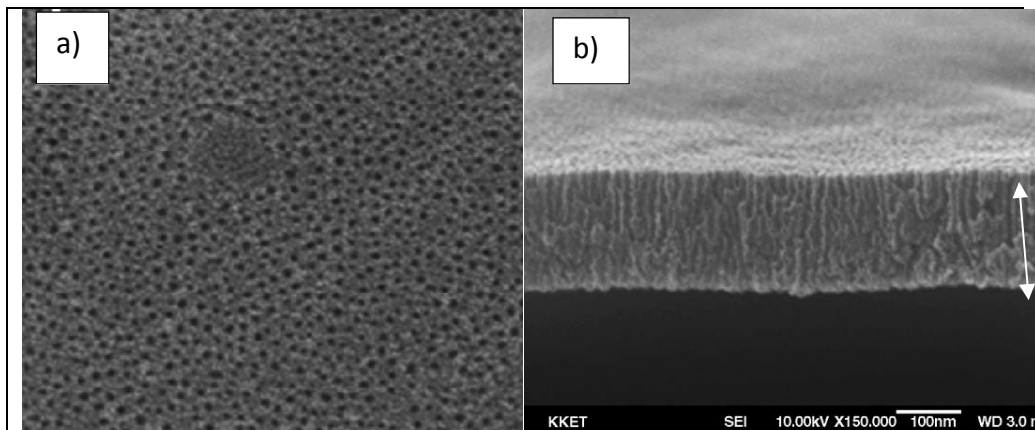


FIGURE 7.4

FE-SEM images of porous niobium oxides prepared in 0.5 M HF + 1 M H_3PO_4 by anodization–annealing–anodization process; a) top view b) sectional profile^[16]

A unique feature in comparison with other anodic metal oxides mentioned above is that the growth of the compact ZrO_2 layer at room temperature directly leads to a crystalline film rather than an amorphous film as observed from other anodic metal oxides (figure 7.5). ZrO_2 is an important functional material that plays a key role as an industrial catalyst and catalyst support^[17].

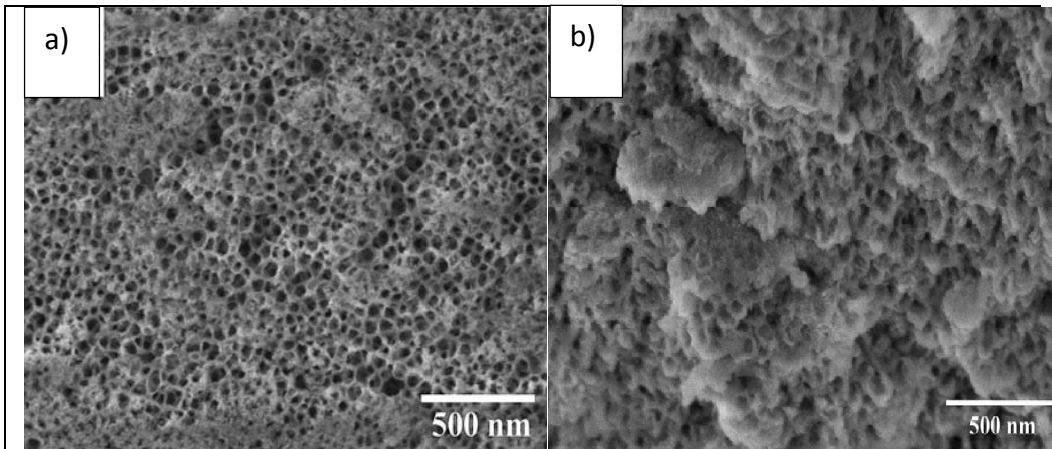


FIGURE 7.5

SEM images of anodic porous zirconium oxide layers formed in 1 M H_2SO_4 + 0.05 M NH_4F electrolyte at 30V for 5 h at 20°C ; a) Plan view b) cross-sectional view^[17]

Anodic aluminium oxide (AAO), was first reported 50 years ago and is now commercially available because its pores can be used as template for preparing various nanoparticles, nanowires and nanotubes. This book chapter presents a review of important developments of these materials including anodization process, formation mechanisms of the pores, factors affecting the process and applications.

Anodic Aluminium oxide

Depending on several factors, in particular the electrolyte, two types of anodic films can be produced. Barrier type films can be formed in completely insoluble electrolytes ($5 < \text{pH} < 7$), e.g., neutral boric acid, ammonium borate, tartrate, and ammonium tetraborate in ethyleneglycol. Porous type films can be created in slightly soluble electrolytes such as sulfuric, phosphoric, chromic and oxalic acid^[18].

Nanoporous alumina films (AAO) are aluminium oxide films consisting of nanosized cylindrical pores arranged parallel to each other in a quasi-hexagonal arrangement. Such templates have been intensely researched due to their wide-spread application in nanofabrication^[19]. The templates are prepared by means of an anodizing process the electrochemical oxidation of aluminium film in an acid under dc conditions^[20].

The pore formation during the anodizing process varies with the electrolyte type, concentration, temperature and applied anodizing potential. Depending on the combination of these parameters, different pore sizes and interpore distances can be achieved. The nanostructure is well defined and has a highly ordered nano-architected that enables these structures to be used as templates^[21].

There are several advantages of AAO membranes, including high porosity and uniform pore size from 5 up to 300 nm, high hydraulic conductivity (water permeability), uniform distribution of pores less than (1% variation), excellent pore structure and high resistance to chemical and temperature degradation. One of the greatest advantages of template based synthesis for the growth of nanotubes and nanotube arrays is the independent control of the length, diameter, and

the wall thickness of the nanotubes. While the length and diameter of resulted nanotubes are dependent on the templates used for the synthesis, the wall thickness of nanotubes can be readily controlled by the growth duration. Another great advantage of template-based synthesis is the possibility of multi-layered hollow nanotube or solid nanocable structures formation^[22].

Types of anodic oxides of aluminium

As indicated in figure 7.7, there are two major types of anodic aluminium oxide film which are porous type oxide film and barrier type oxide film^[23].

Barrier anodic oxides of aluminium

"Barrier-type films" are formed in weak or basic electrolytes in which almost all of the aluminium that electrochemically reacts is converted to aluminium oxide with very little or no dissolution into the electrolyte, e.g. neutral boric acid, ammonium borate, tartrate, ammonium tetra borate in ethylene glycol and organic electrolytes such as glycolic or malic acid.

A characteristic of barrier-type oxide films is that the thickness of the oxide is not affected by the electrolyzing time or temperature of the electrolyte, but only affected by the applied voltage (about 1.4nm.V-1). If the voltage is fixed, the total current for barrier oxide formation decreases exponentially due to the increasing resistance to migration and diffusion of anions and cations through the oxide. The maximum thickness of the barrier oxide is restricted by the oxide breakdown at high voltages, typically around 500-700V^[24].

Porous anodic oxides of aluminium

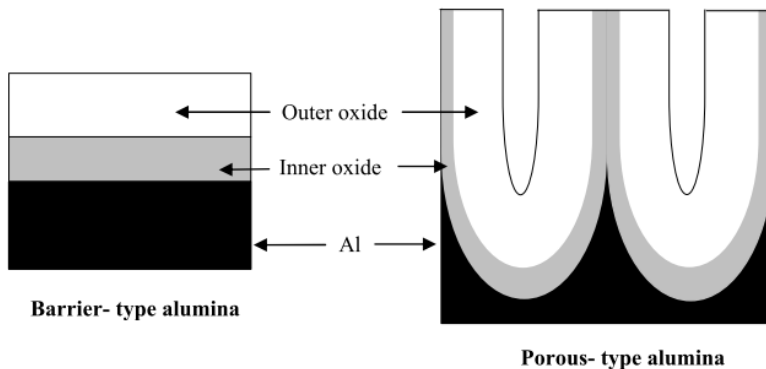
The porous alumina oxide layer is a regular self-organized porous nanostructure formed when aluminium is anodized in slightly acidic conditions, typically with pH less than 5. Porous anodic aluminium oxide film is formed in mild acidic solution.

Unlike barrier oxide film, porous aluminium oxide thickness is dependent on anodization time, voltage, current density, electrolyte temperature, type and concentration. Furthermore, maximum thickness of barrier type oxide film is much less that can be achieved by porous oxide type film. Porous anodic aluminium oxide can be achieved when aluminium is being anodized in mild acid solutions like sulfuric acid, phosphoric acid, oxalic acid, chromic acid, etc. and each acid results porous film of pore diameter different from the other. Pore diameter of anodization in phosphoric acid is bigger than that of anodization in oxalic acid pore diameter of anodization in oxalic acid is bigger than that of anodization in sulfuric acid^[25]. A comparison between properties of barrier type AAO film and properties of porous type AAO film is demonstrated in table 7.1^[25].

TABLE 7.1Comparison between aluminium barrier and porous oxides^[25]

Property	Barrier-type oxide	Porous-type oxide
Structure	Thin, compact, non-porous	Inner layer- thin, compact barrier-type
Thickness	1.4 nm/V	Inner layer - 1 nm/V Varies with current density/voltage, pH and type of electrolyte
Anionic impurity content	1-2%	Up to 17 % ; varies with pH, electrolyte, temperature and current density/voltage
Water content	2.5%	Up to 15% ; varies with pH and electrolyte
Current efficiency for oxide formation	>90%	< 70-80%
Current efficiency for dissolution	< 10%	> 20-30 %

As indicated in figure 7.7, anodic aluminium oxide layer (barrier or porous) resulted from anodization process is consisted of two parts called inner oxide and outer oxide, and this inner and outer oxides are due to the non-homogeneity in anionic content across the film thicknesses^[23].

**FIGURE 7.7**Schematic diagram of (left) barrier type alumina and (right) porous type alumina^[23]

Types of anodization process

Mild anodization

The fabrication of self-ordered Al₂O₃ pore arrays, under conventional so-called 'mild anodization' conditions, requires several days of processing time and the self-ordering phenomenon occurs only in narrow process windows, known as 'self-ordering regimes with specific values of the interpore distance (D_{int}), such as 25 V in 0.3 M H₂SO₄ at 0 °C with $D_{int} = 63$ nm. Owing to the slow oxide growth rates (for example, 2–6 $\mu\text{m}\cdot\text{h}^{-1}$), mild anodization processes based on Masada's approach have not been used in industrial processes so far. For practical applications, simple and fast fabrication of

highly ordered AAO with a wide range of pore sizes and interpore distances would be highly desirable^[26].

Hard anodization

Hard anodization is conducted in conditions similar to low temperature conditions of mild anodization but higher voltages or higher current density and this resulted in higher rate of oxide growth, typically 50 – 100 $\mu\text{m}\cdot\text{h}^{-1}$, of anodic porous aluminium oxide. Because of the higher anodization voltages in hard anodization, very rapid heat generation created across the oxide barrier layer was difficult to be dissipated quickly and this causes many macroscopic burns and cracks observable by the naked eye, and furthermore may cause disordered pore arrangements^[26]. To solve these problems, Lee et al.^[25] first conducted anodization under mild anodizing for several minutes to generate a protective oxide layer and then gradually increase the voltage to the target high voltage of hard anodizing, and as a result macroscopic burns or cracks were eliminated. However, under hard anodizing with H_2SO_4 electrolyte, macroscopic corrugations were found to extend across the entire surface of the alumina sample, indicating the possibility of plastic deformations in the porous alumina or Al substrate. Thus, fast and mechanically stable fabrication of anodic porous alumina with self-ordered pore arrangement is still a challenge.

Terminologies related to porous film characterization

Typical 3-D porous layer cross section and top view are shown in Figure 7.8 pore diameter (d_p) is the mean diameter of each single pore in the entire structure, interpore distance (d_{int}) is the distance between the centers of two adjacent pores, and wall thickness (w) is the distance between the pore edge and the cell edge, barrier layer thickness (B) is the distance between the pore lowest point and the aluminium surface, and porous layer thickness or pore depth (L_p) is the distance between the pore top or film surface and the lowest point in the pore bottom. The parameters of porous alumina and calculation formula are illustrated in table 7.2^[27,28].

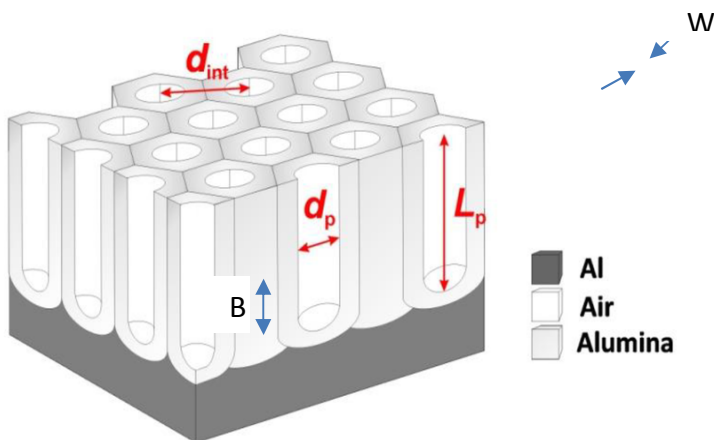


FIGURE 7.8
Idealized structure of anodic porous alumina^[28]

TABLE 7.2Parameters of porous alumina and calculation formula^[27,28]

Parameter	Calculation Formula
Pore diameter (D_p)	$D_p = \lambda_p U$ Where λ_p is the pore proportionality constant = 0.9 nm per volt, U denotes an anodizing potential (V).
Interpore distance (D_c)	$D_c = \lambda_c U$ λ_c is inter pore proportionality constant = 2.5 nm per volt
Wall thickness (W)	$W = \frac{1}{2} (D_c - D_p)$
Thickness of the barrier layer (B)	$H_2SO_4 \rightarrow B = 1.33 W$ $H_2C_2O_4 \rightarrow B = 1.12 W$
Porous layer porosity (α)	$\alpha = \frac{\pi}{2\sqrt{3}} * \left(\frac{D_p}{D_c}\right)$
Pore density (n)	$n = \frac{2 * 10^6}{\sqrt{3} * D_c^2}$

Thermodynamics of aluminium anodizing process

Aluminium also readily reacts with water in aqueous environments, but yields various stable by-products including Al_2O_3 and $Al_2O_3 \cdot 3H_2O$, aluminium ions (Al^{3+}), and aluminate ions (AlO_2^-). For the Al-water system, 6 reactions are known to occur, assuming the absence of complexing agents with Al. For example, Al forms its oxide with water by,



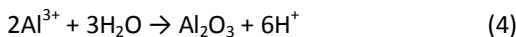
The other 6 reactions are:



At the metal/oxide interface, Al^{3+} ions form and migrate into the oxide layer:



The Al^{3+} ions migrate outwards under the electric field across the oxide from the metal/oxide interface toward the oxide/electrolyte interface:



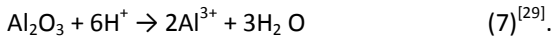
At the oxide/electrolyte interface the water-splitting reaction occurs:



The O^{2-} (oxide) ions migrate inwards under the electric field across the oxide from the oxide/electrolyte interface toward the metal/oxide interface, to form Al_2O_3 :



In the acidic electrolyte where the oxide is soluble, the film dissolution happens:



The formation of aluminium oxide from aluminium is thermodynamically favourable in an oxygen ambient, even at room temperature. The spontaneous reaction of oxidation of Al is driven by a large negative Gibb's free energy change during oxidation.



From the Nernst equation, the equilibrium equation of the reaction (1) is given as a Function of electrode potential E and pH of the solution by;

$$h = 10^{-7} \cdot B_U \cdot V_p - \frac{i.t.M_{Al}}{n.F.\rho_{Al_2O_3}} (1 - T) \quad (10)$$

Where E is the standard reduction potential, R is the universal gas constant, T is the absolute temperature, z is the charge number of the electrode reaction (in this case, z = 3), and F is the Faraday constant (96,500 C/mol) ^[29].

Formation and growth mechanism of anodic porous aluminium oxide

Although aluminium anodization was used successfully and widely for many decades in fabrication of high-ordered nanostructures, it remains unclear and no certainty about factors affecting pore ordering and also influence of initial aluminium surface features on pore ordering ^[30].

Many decades ago, for pore initiation and development, many theories have been put to help understanding of how pores are being initiated and developed. In 1939, Bauman^[31, 32] proposed initiation of pores begins with preformed barrier layer breakthroughs and pore growth proceeds by local oxide dissolution of previously formed breakthroughs. In 1953, Keller^[33] proposed that oxide dissolution happens in homogenous barrier layer formed at the beginning of the anodization process causing current breakdowns and followed by current repair. As a result of the passing current through the oxide layer, local temperature increases and enhances oxide dissolution forming pores. By the time, oxide dissolution proceeds causing pore depth to increase.

In 1961, Akahori ^[34] postulated that after barrier layer and pore formation, local temperature at the pore bottom increases so much, due to passage of current, causing electrolyte at the pore bottom to evaporate and aluminium beneath the oxide layer to melt. He postulated that oxide formation takes place when oxygen forms in the gaseous electrolyte and diffuses into the oxide layer towards the molten aluminium to react with it and form aluminium oxide.

Now, It is generally accepted that pore development and growth is dependent on field assisted dissolution happens to barrier layer formed on aluminium at the start of anodization and this is due to electric current passes, bond between aluminium oxide atoms became weaker, and under acid attacking action oxide dissolution takes place in a rate more than oxide formation, so that pores grow in depth and oxide film grows in thickness^[35].

Two typical regimes are applied for aluminium anodization and porous alumina membrane fabrication. These two regimes are constant potential and constant current regimes. The typical current density-time and potential-time transient records for aluminium anodization process are shown in Figure 7.9. When constant voltage anodization regime is applied for porous alumina growth, the records of current density show a decreasing in values during stage (a), and this is due to formation of high resistance alumina barrier layer. Then breakdowns begin to form on the barrier layer surface declaring the end of stage (a), and beginning of stage (b). Breakthroughs form conductive paths (little pits) for current passing, so steepness of decreasing in current density begins to decrease in stage b till reaching the local minima and then readings start to increase with time. Pits begin to be initiated and grow deeper and wider till they become pores; growth happens in different orientations showing increasing in current density in stage (c). Pits grow till a certain extent after which a rearrangement of pore orientation must take place, to reach the lowest free energy state of the system, orienting pores in parallel orientations. This arrangement corresponds to a local maximum at the ending of stage (c). Then equilibrium is reached between oxide formation and oxide dissolution rates causing pores to grow deeper and keeping current density almost constant with time and this corresponds to stage (d)^[30].

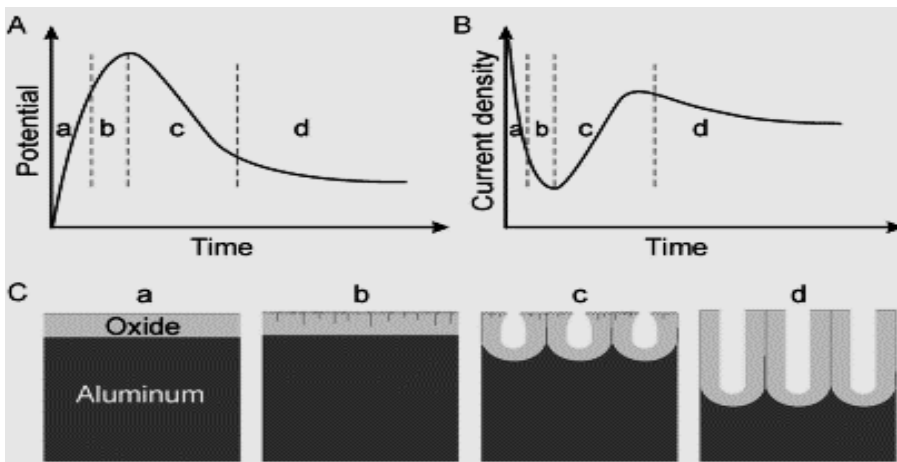


FIGURE 7.9 Typical aluminium anodization process; showing constant current and constant voltage regimes^[30]

Field-assisted dissolution model

In this model, anodization of aluminium surface causes surface roughness to disappear and smoothing of the surface takes place. Sub-grain boundaries, ridges, troughs or any other surface discontinuity as well as surface defects due to electrochemical polishing or etching and also impurities can cause non-uniformity in current distribution across the surface and consequently causes field-assisted dissolution of oxide and local thickening^[36] (as shown in Figure 7.10)^[37, 38].

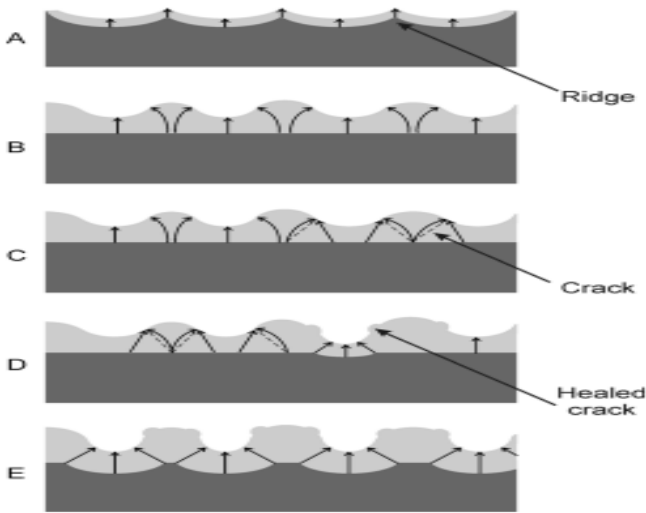


FIGURE 7.10

Current distribution across the non-continuous surface during pore initiation and pore growth as proposed by field-assisted dissolution theory^[37,38]

Thermally-assisted dissolution model

It is well understood that oxide formation is an exothermic reaction which cause local temperature raising, and when temperature increases the oxide dissolution tendency increases, and the high electric field concentration at the pore bottom^[36] as shown in Figure 7.11. The oxide dissolution is assisted by applied electric field due to that when electric field is applied, a polarization happens in the Al-O bond in the oxide and this weakens the bond and make it easier to be broken under the chemical effect of the electrolyte along with joule heating effects and hence this case is called thermally-assisted field-accelerated oxide dissolution^[39]. The growth of the pores proceeds by ions migration. There are two types of ions migration which are inward ions migration and outward ions migration. Inward ions migration takes place from oxygen-carrying ions like O^{2-} and OH^- ions coming from electrolyte inward towards oxide/metal (o/m) interface and outward ions migration takes place from aluminium positive ions going outward towards oxide/electrolyte (o/e) interface. Anions are coming from electrolyte anions in different ways of interaction as shown in Figure 7.12. The ions contribution to porous alumina growth depends to a great extent on the relative transport number between cations and anions, i.e Al^{+3} and O^{2-}/OH^- ions, which are about 0.4 and 0.6, respectively^[40]. The percentage of Al^{+3} and O^{2-} ions participating in oxide formation is about 70% and the rest dissolves in electrolyte^[41].

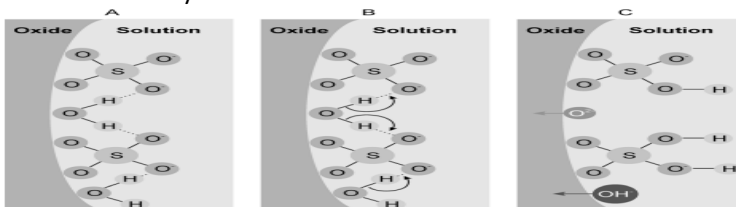


FIGURE 7.11

O^{2-}/OH^- ions formation at electrolyte/oxide interface from water interaction with $[SO_4]^{2-}$ anions adsorbed on the surface^[40]

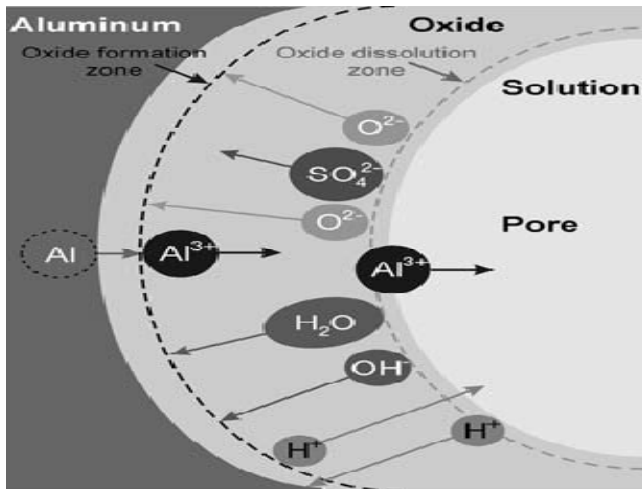


FIGURE 7.12

Ions movement and oxide dissolution mechanism of oxide in sulfuric acid^[36]

Mechanical energy direction model

The previously mentioned model is dependent on cations and anions movement, and oxide formation takes place at electrolyte/oxide interface as well as oxide/metal interface. Almost 60% of the oxide formation takes place at metal/oxide interface where anions (O^{2-}/OH^-) ions combines with aluminium metal and form aluminium oxide and dissolution of oxide layer takes place at electrolyte/oxide interface^[42]. As a result of this ions migration, the model seems to have a mechanical energy parts as movement is essential in process proceeding.

Al³⁺ Direct ejection model

Oxygen isotope (O^{18}) studies indicated that the pore formation does not take place through a simple oxide dissolution process, and suggested that pore formation consists of some kind of oxide decomposition through the direct ejection of Al^{3+} into the solution and the oxide formation at the m/o interface through oxygen transport. This overall reaction is called Al^{3+} direct ejection. It must be noted that while the direct ejection of Al^{3+} ions model is not directly related to pore formation, it is generally believed as a necessary condition for porous oxide formation. In other word, any initiated pores would be healed without the Al^{3+} direct ejection mechanism due to preferential formation of Al_2O_3 at the o/e interface because of the high E-field at the initiated pore base^[43].

Field-assisted plastic flow model

This model indicated that flow of oxide materials has a major role in forming pores, contrary to expectations of a dissolution model of pore development. The flow of the oxide was suggested to arise from the field-assisted plastic flow of oxide materials from pore base toward the cell boundary and the generation of stress due to electrostriction and the oxidation of aluminium. This flow-based pore formation mechanism has been further supported by theoretical study. The unexpected Nd and Hf tracer distribution was attributed to the faster migration rate of the tracer

atoms compared with that of Al^{3+} ions, but it should also be noted that researchers have indicated that a tracer study alone cannot yield sufficient evidence to prove oxide flow or disprove electric-field-assisted dissolution as the mechanism for pore formation^[43].

Other models of porous alumina formation

Shimuzu et al^[38] considered the pore initiation process as a transition from a barrier-type film to a porous-type film due to cracking of film under tensile stress as a result of Pilling Bedworth ratio "PBR" values less than 1. They concluded that the build-up of tensile stress in the oxide contributed to local cracking of the film above pre-existing metal ridges (from electropolishing) on the metal surface. They also suggested that the cracked regions are repaired by oxidation processes; however this leads to non-uniform film growth^[44].

Steady state growth: It is generally accepted for steady-state film growth that oxide nanopores are generated as results of a dynamic equilibrium between the rate of field-assisted oxide dissolution at the electrolyte/oxide (e/o) interface and the rate of oxide formation at the metal/oxide (m/o) interface, which keeps the thickness of the barrier layer constant^[39].

Kinetics of Oxide Formation and Oxide Dissolution

A wide variety of methods were employed to measure the thickness of the oxide layer formed by anodization of aluminium. Recently, optical and microscopic techniques including TEM or SEM have mainly been used to evaluate anodic oxide layer thickness.

For the constant current density anodization, the total thickness of the oxide layer "h" can be calculated from the pore-filling method,

$$h = 10^{-7} \cdot B_U \cdot V_P - \frac{i \cdot t \cdot M_{Al}}{n \cdot F \cdot \rho_{Al_2O_3}} (1-T) \quad (10)$$

where, B is the barrier layer thickness per volt (nm /V), i is the current density (mA/cm^2), M_{Al} is the atomic weight of aluminium, n is the number of electrons associated with oxidation of aluminium, F is Faraday constant, k is the weight fraction of aluminium in alumina (0.529), $\rho_{(Al_2O_3)}$ is the density of porous alumina ($3.2 \text{ g}/\text{cm}^3$), T (Al^{3+}) is the transport number of Al^{3+} ions (about 0.4), and Vp and t are the voltage and time, respectively measured at the point where two straight parts of the voltage–time transient meet.

The thickness of the oxide layer can be calculated from Faraday's law. As the efficiency of anodizing is not usually 100%, the recorded current density cannot be used simply for theoretical estimation of the grown oxide layer, η is the current efficiency should be considered as follows:

$$m_{Al_2O_3} = K_{Al_2O_3} \cdot j \cdot t \cdot \eta = \frac{M_{Al_2O_3}}{zF} \cdot j \cdot t \cdot \eta \quad (11)$$

where, $m_{(Al_2O_3)}$ is a mass of formed oxide, $k_{Al_2O_3}$ is the electrochemical equivalent for aluminium oxide, j is the passing current (A), t is the time (s), η is the current efficiency, $M_{(Al_2O_3)}$ is the molecular weight of aluminium oxide (g/mol), z is the number of electrons associated with oxide formation, and F is Faraday's constant.

Taking into account that the oxide mass can be expressed as the product of oxide density ($\rho_{Al_2O_3}$) and oxide volume ($V_{Al_2O_3}$) or as the product of density, the surface area (S) and oxide height (h):

$$m_{Al_2O_3} = \rho_{Al_2O_3} \cdot V_{Al_2O_3} = \rho_{Al_2O_3} \cdot S \cdot h \quad (12)$$

The oxide layer thickness formed at constant current anodizing is:

$$h = \frac{M_{Al_2O_3}}{z \cdot F \cdot \rho_{Al_2O_3}} \cdot \frac{j}{S} \cdot t \cdot \eta = \frac{M_{Al_2O_3}}{Z \cdot F \cdot \rho_{Al_2O_3}} \cdot i \cdot t \cdot \eta \quad (13)$$

Influence of electrochemical conditions on porous anodized alumina

There are several anodizing parameters such as voltage ^[46, 47], time ^[48], temperature ^[49, 50], composition of electrolyte ^[51], that can affect the pore size and pore arrangement of alumina.

Anodization voltage

According to many authors, anodization voltage is the key parameter that affects all the characteristics of porous membrane as pore diameter, inter-pore distance or cell diameter are linearly proportional to anodizing voltage. According to Araoyinbo et al. ^[45], the anodization process was carried out at ambient temperature with voltage range of 20V to 80V. At every voltage increment there was a significant increase in current density, as well as increase in the nano pore size from about 40nm to 300nm. The data obtained by Stepiński W. J. et al ^[52] has shown that the pore diameter increases with potential, temperature and time of anodization, while the inter pore distance is influenced solely by the potential. Temperature and time changes do not affect the inter pore distance. Porosity is also influenced by potential, temperature and duration of anodization. Pore density is influenced only by the potential ^[53]. Ragab M.A. ^[54], studied the effect of anodizing voltage on the pore diameter and interpore distance of aluminium sheet anodized in 0.6 M sulfuric acid. The obtained pore diameter was 29, 33, 43 nm for anodizing voltage 15, 20, 25 volt, respectively (Figure 7.14).

Electrolyte concentration

Anodization electrolyte concentration is one of the most crucial parameters that affect the final porous membranes' characteristics. As anodization concentration increases, solution becomes more acidic and so solution's chemical action becomes more vigorous, and so attacking of electrolyte to pores' walls becomes stronger, and so pore diameter increases ^[37], in addition to that, increasing electrolyte concentration decreases threshold potential for a field-assisted dissolution of oxide, and oxide formation as well, at pore bottom. Also a result of increasing electrolyte concentration is inter-pore distance decreasing ^[39].

Electrolyte temperature

Anodization electrolyte temperature is one of the most crucial parameters that affect the final porous membranes' characteristics. When Aluminium is being anodized, aluminium turns into aluminium oxide releasing a considerable amount of heat that in turn increases local temperature

at inner oxide layer. So as electrolyte temperature increases, the reaction shifts to backward direction according to Le Chatelier principle towards Al_2O_3 dissolution, so increasing electrolyte temperature, enhances alumina dissolution and enhances pore diameter increasing. The effect of electrolyte temperature effect on different porous membranes' characteristics has been carried out and it was found that in case of constant potential regime, inter-pore distance stays unchanged in case of oxalic acid^[55] and increases in case of sulphuric and phosphoric acids, typically inter-pore distance increased by 8 – 10 % by increasing temperature from -8 or 1 °C up to 10 °C^[56].

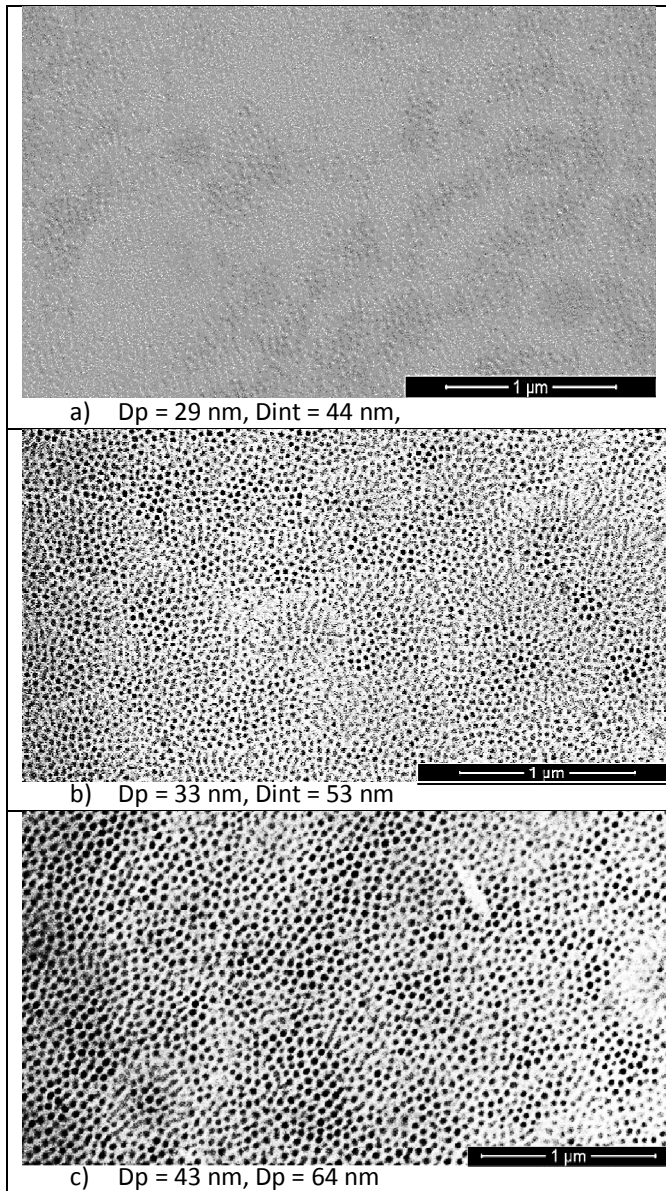


FIGURE 7.14

FESEM images of anodized aluminium showing effect of anodizing potential on pore diameter and inter-pore distance using 0.6M sulphuric acid at temperature 9°C: a) 15V, b) 20V and c) 25V^[54]

Electrolyte type variation

Anodization solution type is the main parameter that determines the pore diameter range and inter-pore distance and also determines the working voltage that must be used to achieve porous alumina membrane^[49]. Sousa C.T. et al.^[56] investigated nanoporous self-organized AAO templates, where both the anodization steps were carried out in 0.3M H₂SO₄ at voltages 15V, 20V and 25V, for 2h, at temperature $12 \pm 2^\circ\text{C}$ ^[56]. The results of this research are an applied potential of 25V giving the best conditions for the appearance of organized patterns. The anodization at 25V gave the largest interpore distance in the aluminium (~30 nm).

J. Martín et al.^[57] used a phosphoric acid/methanol/water mixture (1:10:89, weight proportions) electrolyte, and anodised under a constant potential of 195V and at -4°C , using two steps anodizing process. The results were pore diameter 137nm and interpore distance 447 nm.

Electrolytes such as citric acid, chromic acid and tartaric acid, have also been used with varying success elsewhere^[58]. In summary, the relationship between the conditions for fabrication AAO templates in common electrolytes are given in Table 7.3.

TABLE 7.3

Structural features of nanostructure obtained by anodizing in various conditions^[59]

Electrolyte	Voltage(V)	Pore diameter (nm)	Inter-pore(nm)
Phosphoric acid (H ₃ PO ₄)	100-195	30-80	15-25
	130-250	40-100	15-25
Oxalic acid (H ₂ C ₂ O ₄)	250-500	80-200	60-70
Sulphuric acid (H ₂ SO ₄)			

Electrolyte stirring velocity

During anodization process, hydrogen gas evolves at cathode and oxygen is oxidized at anode causing concentration of hydrogen ions in solution around cathode (catholyte) and concentration of oxygen and hydroxide ions in solution around anode (anolyte) to decline as we go far from the electrodes forming a concentration gradient around the two electrodes. When these ions decline, the total number of charge carriers around the two electrodes decrease, so current readouts increase. In order to avoid this and reach homogenization of the electrolyte in all regions, we have to stir the electrolyte using for example magnetic stirrer. As electrolyte stirring velocity (in rpm) increases, homogenization of electrolyte becomes better^[39].

Electrolyte pH

The influence of electrolyte pH is so far analogous to electrolyte concentration as acid concentration decreases, pH increases. The effect of increasing the electrolyte pH is that it causes a decreasing in dissolution current density as it causes decreasing in the electric field (V/nm) due to reducing the aggressiveness of the electrolyte and so an increase in the barrier layer thickness is resulted. Increasing electrolyte pH causes a decrease in incorporated anionic species in the oxide film^[29] and a slight decrease in porosity is observed^[39].

Applications of Porous Anodic Alumina

Anodic porous alumina which exhibits a characteristic nano-honeycomb structure has received increasing attention both experimentally and theoretically. Due to the quasi-periodic arrangement of the nanopore channels, narrow distribution of pore sizes and interpore distances, relative ease to control the porous scales and self-ordering qualities by anodization conditions, excellent thermal stability, and very low cost, anodic porous alumina has been extensively used as templates for fabrication of various nanostructured materials such as nanodots, nanowires, nanotubes, and many other types, especially to realize the collective functioning of arrays of nano-elements which may not be realized by individual nano-elements, for applications in high density magnetic media, photonic crystals, semiconductor devices, lithium-ion batteries, solar cells, nanocapacitor, etc.^[60].

Nanotechnology applications

Recently, the research on self-organization in nanotechnology has gained momentum with the use of porous anodic alumina. 1-D materials such as nanowires or carbon nanotubes have already shown great promise in applications for quantum devices. By using AAO, researchers have been able to fabricate an inexpensive, high throughput and easily tunable template. Anodized porous alumina has several advantages in the effort to produce Carbon Nanotubes (CNTs). Primarily, they offer consistently parallel pore channels, the ability to engineer varying pore diameters, are optically transparent in the visible spectrum and are resistant to most chemicals except for strong bases and acids. CNTs in AAO have been explored by several groups. The potential applications in electrochemical devices, quantum wires and electrodes for rechargeable Li-batteries are just some of the numerous areas that have been explored. The optical properties of AAO have been well documented and the material has been utilized in both polarizers and electroluminescent devices. The photoluminescent (PL) properties of AAO are further enhanced when they are filled with semiconductor composites such as CdS or ZnO. These optical nanowires are being utilized in polymer light emitting diodes (PLEDs) and optical displays^[19].

Humidity sensors and biosensors

Due to its hydrophilic properties, AAO is currently used in micro humidity sensors that show good response and are easily fabricated. These devices are based on integrated electrodes that take advantage of the sensitive capacitance-humidity relationship. Another interesting characteristic of AAO is its biological properties, and for years, AAO has been used in dental and bone implants due to its biocompatibility and ease of integration with medical implant. Furthermore, these AAO membranes are now employed as electrochemical biosensors. The membrane acts as a support for enzymes and other biological materials^[61].

MEMS and RF applications

To date, for RF and microwave applications, AAO has been used mainly as an isolation layer in multilevel circuits. In AAO was formed on a glass substrate to produce Multichip Module Deposited (MCM-D) substrates. In this process, they were able to fabricate several interconnecting layers of porous and barrier layers of AAO as shown in Figure 7.7. The measured resistance of the layer insulation dielectric layer was on the order of $10^9 \Omega \cdot \text{cm}$ much, higher than porous Si at $10^6 \Omega$ ^[62].

Energy storage

Energy storage devices such as capacitors can store energy in the form of surface charge in their conducting electrodes. Also energy can be stored in electrochemical double layers in ultra-capacitors^[62]. Due to the large surface area provided by nanomaterials, energy storage became much larger than those conventional capacitors^[64]. Energy storage capacity of metal-insulator-metal (MIM) electrostatic capacitors using porous anodic aluminium oxide as insulating material showed a significant increase up to 100 times over the nonporous structured devices^[54]. Moreover, as surface topography of the porous alumina insulator becomes very smooth, energy storage capacity increases and breakdown electric field of the metal-insulator-metal capacitor increases to values approach intrinsic dielectric strength of alumina^[64].

Lithium-ion micro-batteries

Lithium batteries composed of nanowire arrays as anode show much higher energy capacity compared with conventional thin film batteries, due to the large surface area and a reduced Li-ion diffusion length. With the length of nanowire increasing, the capacity can be further increased. However, due to the agglomerate of the high aspect-ratio nanowires, the total surface area decreases, and significant degradation of performance was found^[5].

Conclusion

Aluminium and other nonferrous metals, such as magnesium and titanium are ideally suited to anodizing. Nanoporous alumina AAO films produced during electrochemical anodizing of aluminium has been studied for many years, and has continued to attract interest from various researchers because of its unique chemical and physical properties. These unique properties have made it possible for a wider application such as electronic devices, magnetic storage disks, sensors in hydrogen detection, adsorption of volatile organic compounds, bio devices and in drug delivery, etc.

The pore formation during the anodizing process varies with the electrolyte type, concentration, temperature and applied anodizing potential. Depending on the combination of these parameters, different pore sizes and inter-pore distances can be achieved. The nanostructure is well defined and has a highly ordered nano architecture that enables these structures to be used as templates. There are several advantages of AAO membranes, including high porosity and uniform pore size from 5 up to 300 nm, high hydraulic conductivity (water permeability), uniform distribution of pores less than (1% variation), excellent pore structure and high resistance to chemical and temperature degradation. One of the greatest advantages of template based synthesis for the growth of nanotubes and nanotube arrays is the independent control of the length, diameter, and the wall thickness of the nanotubes. While the length and diameter of resulted nanotubes are dependent on the templates used for the synthesis, the wall thickness of nanotubes can be readily controlled by the growth duration. Another great advantage of template-based synthesis is the possibility of multilayered hollow nanotube or solid nanocable structures formation.

References

1. Su Z. X., and Zhou W., "Porous anodic metal oxides", Science Foundation in China, Vol. 16, No. 1, 2008, pp. 36 – 55.
2. Prathap A.M.U., Srivastava R., Synthesis of nanoporous metal oxides through the self-assembly of phloroglucinol–form aldehydesol and tri-block copolymer, Journal of Colloid and Interface Science, Vol. 358, No. 2, 2011, pp. 399–408.
3. Ou J. Z., Nanostructured transitional metal oxides: Applications in smart windows, optical gas sensors and dye-sensitized solar cells, Ph. D, RMIT University, Australia, 2012.
4. Hoa N. D., Van Duy N., El-Safty Sh. A., and Van Hieu N., Meso-/nanoporous semiconducting metal oxides for gas sensor applications, Journal of Nanomaterials, Vol. 2015, Article ID 972025, 14 pages.
5. Storm J., Chen J. H., Ling X. S., Zandbergen H.W. and Dekker C., Fabrication of solid-state nanopores with single-nanometre precision, nature materials, Vol. 2, 2003, pp. 537-540.
6. Zhu Z., Garcia-Gancedo L., Liu Q., Flewitt A, Milne W., Moussy F., Size-tunable porous anodic alumina nano-structure for biosensing, Soft Nanoscience Letters, Vol. 1, 2011, pp. 55-60.
7. Yao Z., Wang C., Li Y. and Kim N. Y., AAO-assisted synthesis of highly ordered, large-scale TiO₂ nanowire arrays via sputtering and atomic layer deposition, Nanoscale Research Letters, Vol. 10, No. 166, 2015, pp. 1-7.
8. Pickett A. N., Electrospinning applications in mechanochemistry and multifunctional hydrogel materials, M.Sc., University of Illinois at Urbana-Champaign, USA, 2012.
9. Samantilleke A. P., Carneiro J. O., Azevedo S., Thuy T., and Teixeira V., Electrochemical anodizing, structural and mechanical characterization of nanoporous alumina templates, Journal of Nano Research, Vol. 25, 2013, pp. 77-89.
10. Kumeria T., Santos A. and Losic D., Review nanoporous anodic alumina platforms: Engineered surface chemistry and structure for optical sensing applications, Sensors, Vol. 14, 2014, pp. 11878-11918.
11. Eddy G., Poinern J., Ali N. and Fawcett D., " Review progress in nano-engineered anodic aluminium oxide membrane development", Materials, Vol. 4, 2011, pp. 487-526.
12. Dyer C. K., Electrolytic rectification and cathodic charge reversibility of some valve metals, Electrocomponent Science and Technology, Vol. 1, 1974, pp. 121-127.
13. Michaelis A., 2008, Advances in electrochemical science and engineering, (edit.. Alkire R.C, Kolb D. M., Lipkowski J. and Ross P. N.), Vol. 10, Chapter 1; valve metal, Si and ceramic oxides as dielectric films for passive and active electronic devices, WILEY-VCH Verlag GmbH & Co. KGaA.
14. Gong, D. W., Grimes, C. A., Varghese, O. K., Hu, W. C., Singh, R. S., Chen, Z. and Dickey, E. C., " Titanium oxide nanotube arrays prepared by anodic oxidation", J. Mater. Res., Vol. 16, 2001, pp. 3331-3334.
15. Tsuchiya, H. and Schmuki P., "Self-organized high aspect ratio porous hafnium oxide", Electrochem. Commun., Vol. 7, 2005, pp. 49-52.
16. Choi J., Lim, J. H., Lee, J. and Kim K.J., " Porous niobium oxide films prepared by anodization in HF/H₃PO₄" Nanotech., Vol. 18, 2007, Article ID 055603, 6 pages..
17. Tsuchiya H., Schmuki P., Thick self-organized porous zirconium oxide formed in H₂SO₄/NH₄F electrolytes, Electrochemistry Communications, Vol. 6, 2004, pp. 1131–1134.

18. Diggle J. W., Downie T. C, and Goulding C. W., Anodic oxide films on aluminium, *Chem. Rev.*, Vol. 69, No. 3, 1969, pp.365-405.
19. Wu Z., Richter, C. and Menona, L., "A Study of anodization process during pore formation in nanoporous alumina templates ", *Journal of The Electrochemical Society*, Vol.154, 2007, pp.8-12.
20. Eddy G., Poinern J., Ali N. and Fawcett D., "Progress in nano-engineered anodic aluminium oxide membrane development ", *Materials*, Vol. 4, 2011, pp. 487-526.
21. Purkait M.K., Mohanty K., 2011, *Membrane technologies and applications*, CRC Press.
22. Vorozhtsova M., Drbohlavova J. and Hubalek J.,2011, *Microsensors*, (edit. Minin I.), chapter 6; *Chemical microsensors with ordered nanostructures*, Intech.
23. Nielsch K., Choi J., Schwirn, K., Wehrspohn, R. B., Gosele, U., "Self-ordering regimes of porous alumina: The 10% porosity rule", *Nano Letters*, Vol. 2, 2002, pp. 677–680.
24. Krishnan R., "Templated self-assembly of nanoporous alumina: Pore formation and ordering mechanisms, methodologies, and applications", PhD. Thesis, Massachusetts Institute of Technology, United States of America, 2005, pp 43 – 91.
25. Lee W., "The anodization of aluminium for nanotechnology applications", *Journal of Materials*, Vol. 62, No. 6, 2010, pp. 57-62.
26. ASM International, 1994, "ASM Handbook: Surface Engineering", Vol. 5, 9th Edition, pp. 2270 – 2073.
27. Shimizu K., Habazaki H., Skeldon P., Thompson G. E., Wood, G. C., Comparison of depth profiling analysis of a thick, electrolytically-colored porous alumina film by EPMA and GDOES, *Surface and Interface Analysis*, Vol. 27, No.12, 1999, pp. 1046 – 1049.
28. Santos A., Kumeria T., Losic D., Nanoporous anodic alumina: A versatile platform for optical biosensors, *Materials*, Vol. 7, No. 6, 2014, pp. 4297 – 4320.
29. Oh, J., "Porous anodic aluminium oxide scaffolds; formation mechanisms and applications", PhD. Thesis, Massachusetts Institute of Technology, U.S.A, 2010, pp. 21 – 68.
30. Eftekhari A., 2008, "Nanostructured materials in electrochemistry", Wiley-VCH Verlag GmbH & Co. KGaA, pp. 1-111.
31. Baumann W., "Wechselstromuntersuchungen an anodisch oxydiertem Aluminium", *Zeitschrift für Physik*, Vol. 102, 1936, pp. 59 – 66.
32. Baumaun W., "Entstehung und Struktur elektrolytisch erzeugter Aluminiumoxydschichten", *Zeitschrift für Physik*, Vol. 111, 1939, pp 707 – 736.
33. Keller F., Hunter M. S., Robinson D. L., "Structural features of oxide coatings on aluminium", *Journal of the Electrochemical Society*, Vol. 100, 1953, pp. 411–419.
34. Akahori H., "Electron microscopic study of growing mechanism of aluminium anodic oxide film," *Journal of Electron Microscopy*, Vol. 10, 1961, pp. 175 – 185.
35. Thompson G.E., "Porous anodic alumina: Fabrication, characterization and applications", *Thin Solid Films*, Vol. 297, No. 1–2, 1997, pp. 192 – 201.
36. Siejka J., Orteg C., "An O¹⁸ study of field-assisted pore formation in compact anodic oxide films on aluminium", *Journal of the Electrochemical Society*, Vol. 124, No. 6, 1977, pp. 883 – 891.
37. Thompson G.E., Wood G.C., "Anodic films on aluminium", *Treatise on Materials Science and Technology*, Vol. 23, 1983, pp 205 – 329.
38. Shimizu K., Kobayashi K., Thompson, G.E., Wood, G.C., "Development of porous anodic films on aluminium", *Philosophical Magazine A*, Vol. 66, No. 4, 1992, pp 643 – 652.

39. O'Sullivan J.P., Wood, G.C., "The morphology and mechanism of formation of porous anodic films on aluminium", Proceedings of the Royal Society of London, series A-Mathematics and Physical Sciences, Vol. A317, 1970, pp. 511-543.
40. Xu Y., Thompson G.E., Wood G.C., Bethune B., "Anion incorporation and migration during barrier film formation on aluminium", Corrosion Science, Vol. 27, No. 1, 1987, pp. 83 – 93, 95 – 102.
41. Palbroda E., "Aluminium porous growth—II on the rate determining step", Electrochimica Acta, Vol. 40, 1995, pp. 1051 – 1055.
42. Li F., Zhang L., Metzger R.M., "On the growth of highly ordered pores in anodized aluminium oxide", Chemistry of Materials, Vol. 10, 1998, pp. 2470 – 2480.
43. Dong H., "Surface engineering of light alloys Aluminium, magnesium and titanium alloys", Part II, Woodhead Publishing Limited, 2010, pp. 83 – 107.
44. Hunter M. S. and P. Fowle, "Factors affecting the formation of anodic oxide coatings," Journal of the Electrochemical Society, Vol. 101, 1954, pp. 514–519.
45. Araoyinbo .A.O, Noor A.F.M., Sreekantan S. and Aziz A., "Voltage effect on electrochemical anodization of aluminium at ambient temperature", International Journal of Mechanical and Materials Engineering (IJMME), Vol. 5, No. 1, 2010, pp. 53-58.
46. Kim Y.S., Pyun S.I., Moon S.M., Kim, J.D.," The effects of applied potential and pH on the electrochemical dissolution of the barrier layer in porous anodic oxide film on pure aluminium", Corros. Sci. , Vol. 38, 1996, pp.329- 336.
47. Choi Y. C., Hyeon J. Y. , Bu S. D.," Effects of anodizing voltages and corresponding current densities on self-ordering process of nanopores in porous anodic alumina as anodized in oxalic and sulfuric Acids", Journal of the Korean Physical Society, Vol. 55, No. 2, 2009, pp. 835- 840.
48. Bannigidad P., Vidyasagar C. C., Effect of time on anodized Al₂O₃ nanopore FESEM images using digital image processing techniques: A study on computational chemistry, International Journal of Emerging Trends & Technology in Computer Science (IJETTCS), Vol. 4, No. 3, 2015, pp.15-22.
49. Sulka GD, Parkola KG.," Temperature influence on well-ordered nanopore structures grown by anodization of aluminium in sulphuric acid", Electrochimica Acta, Vol. 52, 2007, pp.1880-1888.
50. Belwalkar A., Grasing E., Van Geertruyden W., Huang Z., and Misiolek W.Z., Effect of processing parameters on pore structure and thickness of anodic aluminium oxide (AAO) tubular membranes, J Memb Sci., Vol. 319, No.1-2, 2008, pp. 192–198.
51. Chung C.K. , Liao M.W., Chang H.C., Lee C.T.," Effects of temperature and voltage mode on nanoporous anodic aluminium oxide films by one-step anodization", Thin Solid Films, Vol. 520 , 2011, pp. 1554-1558.
52. Stępniewski W. J., Bojar Z., "Synthesis of anodic aluminium oxide (AAO) at relatively high temperatures. Study of the influence of anodization conditions on the alumina structural features", Surface & Coatings Technology, Vol. 206, 2001, pp 265 – 272.
53. Oh H., Jang K., and Chi C.-S., "Impedance characteristics of oxide layers on aluminium", Bull. Korean Chem. Soc., Vol. 20, No. 11, 1999, pp. 1340-1344.
54. Ragab M. A., "Nano porous Aluminium oxide film fabrication and characterization", MSc. thesis, Faculty of Engineering, Cairo University, Egypt, 2014.

55. Wang W., Tian M., Abdulagatov A., George S. M., Lee Y. C., Yang R. G., "Three-Dimensional Ni/TiO₂ nanowire network for high areal capacity lithium ion microbattery applications", *Nano Letters*, Vol. 12, No. 2, 2012, pp. 655 – 660.
56. Sousa C.T., Leitao D., Ventura J., Pereira A.M., Amado M., Sousa J.B. and Araújo J.P., Nanoporous self - organized anodic alumina templates, Presented in 8^oENCMP Lamego 2007(Portugal).
57. Martín J., Manzano C.V. and Martín-González M., *Microporous and Mesoporous Materials*, Vol. 151, 2010, pp. 311–316.
58. Sulka Grzegorz D., 2008, *Nanostructured Materials*, WILEY-VCH Verlag GmbH & Co. KGaA, Weinheim, pp. 1–116
59. Samatilleke A. P., Carneiro J.O., Alpuim P., Teixeira V. and THUY T.T., 2013, *Nanotechnology Vol. 4: Nanomaterials and Nanostructures*, (edit. Navaani N. K. & Sinha Sh.), Chapter 12; Nanoporous alumina templates: Anodization and mechanical characterisation, Studium Press LLC.
60. Zixue S., "Porous anodic metal oxides ", University of St. Andrews, Scotland, 2009.
61. Hoe S. Y., "Fabrication of Tungsten oxide nanostructured films using anodic porous alumina and application in gas sensing", Godwin, National University of Singapore, Singapore, 2005.
62. Brinda O. T., "Low temperature RF MEMS inductors using porous anodic alumina", University of Waterloo, Canada, 2008.
63. Haspert L. C., Lee, S. B., Rubloff, G. W., "Nanoengineering strategies for metal–insulator–metal electrostatic nanocapacitors", *American Chemical Society Nano*, Vol. 6, 2012, pp 3528 – 3536.
64. Bufon C. C. B., Gonzalez J. D. C., Thurmer D. J., Grimm D., Bauer M., Schmidt O. G., 2010, "Self-assembled ultra-compact energy storage elements based on hybrid nanomembranes", *Nano Letters*, Vol. 10, No.7, 2010, pp 2506 – 2510.